Available online at www.sciencedirect.com
SCIENCE DIRECT
Cancer Letters xx (2005) 1–13
CANCER Letters
www.elsevier.com/locate/canlet

Methyl protodioscin induces G_2/M arrest and apoptosis in K562 cells with the hyperpolarization of mitochondria

Ming-Jie Liu[a], Patrick Ying-Kit Yue[b], Zhao Wang[a,c], Ricky Ngok-Shun Wong[b,*]

[a]*Department of Biological Sciences and Biotechnology, Tsinghua University, Beijing, P.R. China*
[b]*Department of Biology, Hong Kong Baptist University, Kowloon Tong, Hong Kong, P.R. China*
[c]*Institue of Biomedicine, Tsinghua University, Beijing, P.R. China*

Received 6 July 2004; received in revised form 18 November 2004; accepted 22 November 2004

Abstract

Methyl protodioscin is a furostanol bisglycoside with antitumor properties. The present study investigated its effects on human chronic myelogenous leukemia K562 cells. Cell cycle analysis showed that methyl protodioscin caused distinct G_2/M arrest, with the appearance of polyploidy population. The levels of cyclin B1 decreased, whereas Cdc2 kept at a steady level. Subsequent apoptosis after G_2/M blockage was demonstrated through DNA fragmentation and the annexin V staining assay. Methyl protodioscin induced a biphasic alteration (i.e. an early hyperpolarization, followed by depolarization) in mitochondrial membrane potential of K562 cells. The transient decline of intracellular Ca^{2+} concentration was observed at early stage. The generation of reactive oxygen species was also detected. The anti-apoptotic Bcl-x_L transiently increased and then decreased. And the pro-apoptotic Bax was markedly up-regulated. Taken together, these data demonstrated that methyl protodioscin inhibits K562 cell proliferation via G_2/M arrest and apoptosis, with mitochondrial hyperpolarization and the disruption of Ca^{2+} homeostasis playing important roles.
© 2004 Elsevier Ireland Ltd. All rights reserved.

Keywords: Methyl protodioscin; Apoptosis; G2/M arrest; Ca^{2+} homeostasis; Mitochondrial hyperpolarization

1. Introduction

The up-to-date rational drug development in cancer therapy appears to concentrate on the discovery of effective pharmaceutical agents that can intervene diverse signaling pathways [1,2]. The regulatory system that control normal cell proliferation and cell death stay balanced through orchestrated cascades of multiple interacting signaling routes. When this rhythmic scheme is perturbed by biochemical agents, it often results in the breakdown of cell cycle machinery, subsequently entering into apoptosis. Checkpoint molecules establish the timing and strength of arrest, repair or apoptosis responses to the damage [3]. Specifically, it has been reported that the induction of a cell cycle arrest at G_2/M could be attributed to a reduction in CDK1-associated kinase activity that determines entry into mitosis [4]. Molecules regulating cell division, such as cyclin-dependent kinases (CDKs) and inhibitors for

* Corresponding author. Tel.: +852 3411 7050; fax: +852 3411 5995.
E-mail address: rnswong@hkbu.edu.hk (R.N.-S. Wong).

0304-3835/$ - see front matter © 2004 Elsevier Ireland Ltd. All rights reserved.
doi:10.1016/j.canlet.2004.11.051

CDKs, are also implicated in the regulation of apoptosis.

Apoptosis is a highly regulated process of cell suicide, in which mitochondria integrate diverse stimuli into a core intrinsic death pathway [5]. Apoptosis induced by extracellular cues and internal insults such as DNA damage is mainly dependent on mitochondria, with the perturbation of inner membrane as an early event. It may be caused by the opening of the permeability transition pore (PTP), resulting in the decline of mitochondrial membrane potential (MMP, $\Delta\Psi_m$) and the release of pro-apoptotic proteins, such as cytochrome *c* and AIF [6]. Cytochrome *c* then activates caspase cascades to disassemble the structure of the cells [7]. Bcl-2 family members appear to regulate the commitment to survive or die by controlling the integrity of mitochondrial membrane [8]. In the early stage of apoptosis, pro-apoptotic Bax translocates from cytosol to mitochondria, leading to the efflux of cytochrome *c*. Mitochondria also modulate and synchronize Ca^{2+} signaling. Their central function in Ca^{2+}-regulated cell death program was well established [9]. Disruption of intracellular Ca^{2+} homeostasis is a critical event in the initiation of apoptosis [10], leading to mitochondrial Ca^{2+} uptake and Ca^{2+} overloading, which have detrimental effects in terms of enhanced production of reactive oxygen species (ROS). The defects of Ca^{2+}-cycling may also result in the decline of MMP through the opening of the PTP, finally culminating in mitochondrial dysfunction and apoptosis [11].

Diosgenyl saponins comprise a diverse class of plant glycosides that possess a broad range of biological activities. Their sapogenins are secondary metabolites whose biosynthetic precursors are sterols, especially cholesterol. They constitute one of the major components in Chinese herbal medicine, with the various carbohydrate residues being covalently conjugated to the sapogenin backbone. Some of these glycosides have been used to treat malaria, helminthes infections, and snake bites. Others are good antifungal and antibacterial agents. Methyl protodioscin is a furostanol bisglycoside (Fig. 1). It was tested for in vitro cytotoxicity against 60 human cancer cell lines in the NCI's (National Cancer Institute, USA) anticancer drug screen and showed potent activity [12,13]. Recent study found that it has antiosteoporotic activity without side effect on the uterus [14] and it has been totally synthesized from its aglycon diosgenin [15].

Concerning this attractive kind of natural product, it is necessary to study its pharmacological mode of action at cellular and molecular levels. The present study is to investigate the antiproliferative effects of methyl protodioscin on human chronic myelogenous leukemia (CML) K562 cells. The results showed that methyl protodioscin inhibited proliferation via blocking cell cycle progression at G_2/M phase and subsequently progressing into apoptosis. The underlying events relevant to mitochondria were studied in detail, including the alteration of MMP, ROS generation and failure control of Ca^{2+} homeostasis. The involvement of Bcl-2 family members was also demonstrated.

2. Materials and methods

2.1. Cell culture

Human CML cell line K562 was kindly provided by Prof. Li-Sheng Wang (Academy of Military Medical Sciences, Beijing). Human promyelocytic leukemia NB_4 cells were presented by Prof. Zhu Chen (Rui-jin Hospital, Shanghai Second Medical University). Human colon adenocarcinoma cell line HT-29 was obtained from Institute of Medicinal Biotechnology, Chinese Academy of Medical Sciences. These cells were cultured in RPMI 1640 medium (Invitrogen Corporation, CA), with 10% fetal bovine serum (FBS) (Hyclone Laboratories Inc., UT), 100 IU/mL penicillin, and 100 μg/mL streptomycin in humidified air at 37 °C with 5% CO_2.

2.2. Materials

Methyl protodioscin, 3-*O*-[α-L-rhamnopyranosyl-(1→2)-{α-L-rhamnopyranosyl-(1→4)}-β-D-glucopyranosyl]-26-*O*-[β-D-glucopyranosyl]-22-methoxy-25(*R*)-furost-5-ene-3β,26-diol, was isolated from *Polygnotum zanlanscianse* Pamp [16]. It was dissolved in physiological saline (50 μM) and diluted with the fresh medium to achieve the desired concentration. 3-(4,5-dimethyl-thiazol-2-yl)-2,5-Diphenyl-tetrazolium bromide (MTT), 12-*O*-tetradecany-phorbol-acetate

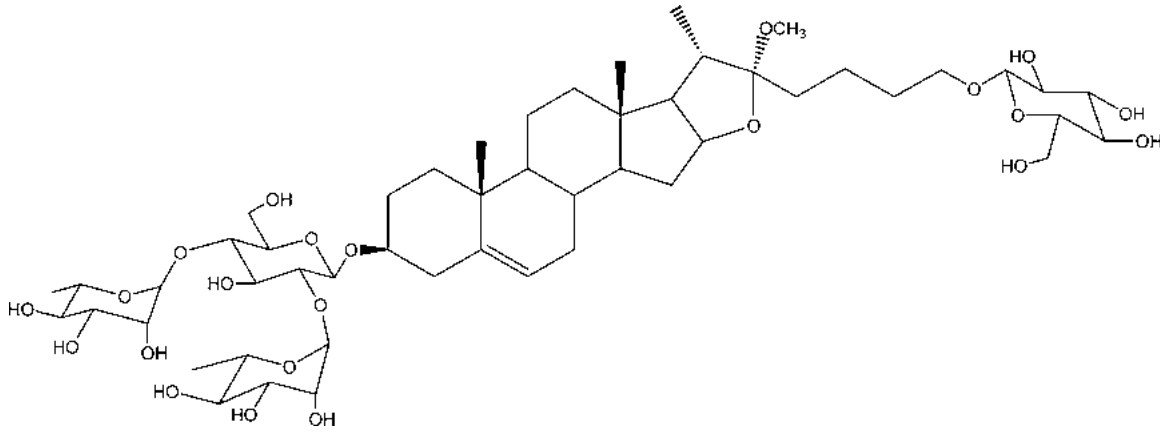

Fig. 1. Chemical structure of methyl protodioscin.

(TPA), Wright-Giemsa stain (modified), propidium iodide (PI), and mouse anti-β-actin monoclonal antibody (McAb) (clone AC-74) were all purchased from Sigma Chemical Co. 4′,6-Diamidin-2′-phenylindoldihydrochloride (DAPI) was purchased from Roche Diagnostics GmbH (Mannheim, Germany). 2′,7′-Dichlorodihydrofluorescin diacetate (DCFH-DA), Fluo-3, and 3′,3′-dihexyloxacabocyanine ($DiOC_6(3)$) were purchased from Fluka Chemie GmbH (Steinheim, Switzerland). Rabbit anti-Bax polyclonal antibody (clone N-20), mouse anti-Bcl-x_L McAb (clone H-5), mouse anti-Cdc2 McAb (clone 17), and mouse anti-cyclin B1 McAb (clone GNS1) were purchased from Santa Cruz Biotechnology, Inc. (CA, USA).

2.3. Cell viability

The cells were suspended at a final concentration of 5×10^4 cells/mL and seeded in 96-well microtiter plates. Various concentrations of methyl protodioscin were added to each well in triplicate. After incubation for the indicated times, the viable cells were counted by trypan blue exclusion method. MTT assay was also employed to measure cell viability. After treatment, the cells were incubated with MTT (0.5 mg/mL) for 4 h. The formazan precipitate was dissolved in 200 μL DMSO and the absorbance at 550 nm was measured by a Benchmark microplate reader (Bio-Rad, CA).

2.4. Cytomorphology

The cells were directly observed under inverted phase-contrast microscopy (Leica DMIRB) and recorded with Leica CCD camera (DC200). Their nuclei were stained with DAPI (10 μg/mL) and examined by fluorescence microscopy (Leica DMIRB and MPS60, Leica Microsystems Wetzlar GmbH). Meanwhile, the cells were centrifuged onto slides by a cytospin (700 rpm, 5 min), stained with Wright-Giemsa dye, and observed under microscopy (Leica DMLB and MPS60).

2.5. Flow cytometric analysis of cell cycle and apoptosis

Cells were fixed by 70% ethanol at −20 °C for at least 12 h. After two washes with phosphate buffered solution (PBS), the cells were incubated in RNase A/PBS (100 μg/mL) at 37 °C for 30 min. Intracellular DNA was labeled with PI (50 μg/mL) and analyzed with a FACSCalibur fluorescence-activated cell sorter (FACS) using CELLQuest software (Becton Dickinson, NJ). The cell cycle profile was obtained by analyzing 15,000 cells with ModFIT LT 3.0 program (Becton Dickinson, NJ). Surface exposure of phosphatidylserine in apoptotic cells was measured by ApoAlert® Annexin V-FITC apoptosis detection kit (BD Biosciences Clontech, CA).

2.6. DNA fragmentation assay

The untreated and treated cells were harvested and lysed in 100 μL buffer (10 mM Tris–HCL (pH 7.4), 10 mM EDTA (pH 8.0), 0.5% Triton X-100). The supernatant was acquired through centrifugation at 14,000×*g* for 10 min, and then incubated with RNase A (200 μg/mL) at 37 °C for 60 min. Proteins were removed by incubation with Proteinase K (200 μg/mL) at 50 °C for 30 min. The lysate was added with 20 μL 5 M NaCl and 120 μL isopropanol. After deposition at −20 °C for 12 h, the precipitated DNA pellet was dissolved in Tris–acetate–EDTA buffer, electrophoresed in a 1.5% agarose gel, stained with ethidium bromide, and photographed under UV illumination.

2.7. Western blot

The cells were harvested and washed with PBS. Their lysates were obtained using lysis buffer (150 mM NaCl, 10 mM Tris (pH 7.4), 5 mM EDTA (pH 8.0), 1% Triton X-100, 1 mM PMSF, 20 μg/mL aprotinin, 50 μg/mL leupeptin, 1 mM benzaidine, 1 μg/mL pepstatin), followed by centrifugation (10,000×*g*, 20 min). Total protein concentration in the supernatant was determined with Bicinchoninic Acid assay (Beyotime biotechnology, China). Proteins were normalized to 50 μg per lane, resolved on 12.5% polyacrylamide gels, and subsequently blotted onto PVDF membranes. After blocking with TTBS (100 mM Tris–HCl, pH 7.5, 0.9% NaCl, 0.1% Tween 20) containing 5% (w/v) skim milk, the membranes were, respectively, incubated with primary and secondary antibodies. Then, the membranes were washed with TTBS and visualized with ECF western blotting kit (Amersham Biosciences). The densities of bands were determined with a fluorescence scanner (Storm 860) and analyzed with ImageQuant software (Amersham Biosciences).

2.8. Measurement of mitochondrial membrane potential

Mitochondrial energization was determined by the retention of the dye $DiOC_6(3)$. About one million cells were harvested and washed twice with PBS. After incubation with 50 nM $DiOC_6(3)$ at 37 °C for 30 min, the cells were washed again and analyzed with FACS.

2.9. Analysis of intracellular Ca^{2+} concentration

The changes of intracellular Ca^{2+} concentration were determined by a fluorescent dye, Fluo-3. Cells were washed twice with RPMI 1640 medium and incubated with 5 μM Fluo-3 at 37 °C for 30 min. Then, the cells were washed and analyzed with FACS.

2.10. Measurement of intracellular ROS

Intracellular ROS production was measured by using a fluorescent dye, DCFH-DA, which can be converted to DCFH by esterases when the cells take it up. DCFH is reactive with ROS to give a new highly fluorescent compound, dichlorofluorescein, which can be analyzed with FACS. The treated cells were incubated with DCFH-DA (10 μM) at 37 °C for 1 h, and then measured with the FACS.

2.11. Statistical analysis

One-way analysis of variance (ANOVA) was performed to determine the significance between groups. A *P*-value of less than 0.05 ($P<0.05$) was considered as statistically significant. All the figures shown in this article were obtained from at least three independent experiments with a similar pattern.

3. Results

3.1. Methyl protodioscin suppresses the growth of tumor cells

K562 cells, human leukemia NB_4 cells and human colon HT-29 cells were treated with different concentrations of methyl protodioscin for different times. MTT assay shows the antiproliferative effects. The IC_{50} (inhibitory concentration 50%) values were about 3, 5, and 1.5 μM, respectively, indicating the susceptibility of HT-29 cells is higher than leukemia cells (Fig. 2A). The viability was also evaluated daily based on the ability of the cells to exclude trypan blue. Methyl protodioscin induced a time- and

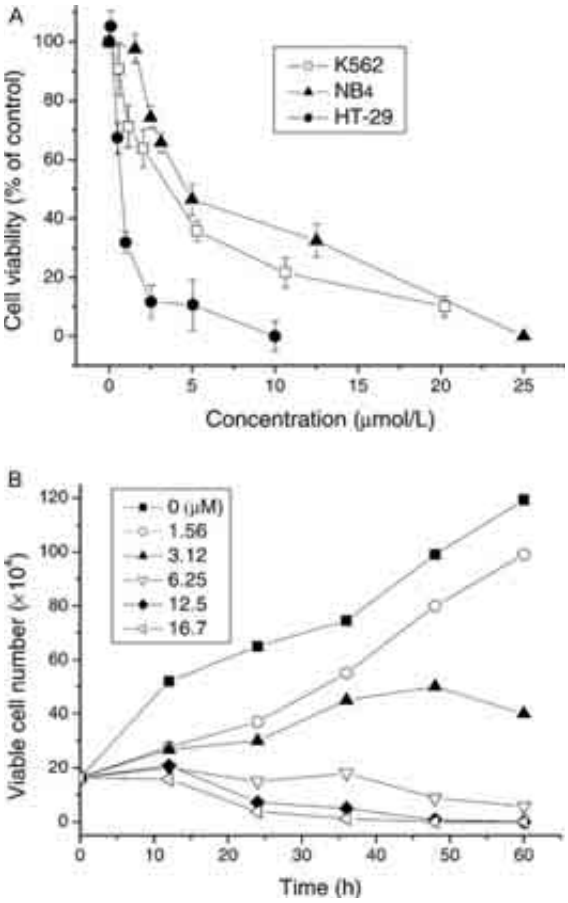

Fig. 2. Effects of methyl protodioscin on the viability of tumor cells. (A) K562, NB_4 and HT-29 cells were treated with methyl protodioscin at the indicated concentrations for 72 h. The viability was determined by MTT assay. Each point is the mean of three replicates; bars represent the standard deviation. (B) The number of viable cells was measured in triplicate by trypan blue exclusion assay. Each point represents the mean of the data from three independent experiments.

dose-dependent diminution of cells, indicating its ability to impair proliferation potential (Fig. 2B).

3.2. Methyl protodioscin induces G_2/M arrest and apoptosis in K562 cells

Fig. 3 shows the representative morphology of K562 cells when exposed to methyl protodioscin (3 μM) for 48 h. The control K562 cells appeared normal features, with the nuclei round and homogeneous (Fig. 3A, C and E). After treatment, the cells exhibited the characteristic features of apoptosis, such as the appearance of apoptotic bodies, chromatin condensation and fragmentation, as indicated by DAPI staining (Fig. 3B and D). In addition, the treated cells showed somewhat larger than control cells in both cellular size and cytoplasmic content. The nuclear complexity was also seen in the slides stained by Wright-Giemsa dye, suggesting that these cells are in a multinucleared state without cell division (Fig. 3F). In order to determine whether K562 cells underwent megakaryocyte differentiation, CD41 expression was detected using TPA as positive control. The results showed that methyl protodioscin was not an inducer (data not shown). The distribution of cell cycle was examined at the indicated times. At a concentration of 3 μM, methyl protodioscin induced a time-dependent increase of G_2/M cell population in K562 cells and polyploidy cells appeared subsequently (Fig. 4A). To determine whether the block of G_2/M progression was transient or permanent, cells were incubated with 2.5 μM methyl protodioscin for 24 h and then transferred to fresh medium. Within 48 h of the removal, the characteristic of cell cycle recovered. Thus the G_2/M blockage is reversible (Fig. 4B).

Fig. 4A also shows a dramatic hypodiploid (sub-G_1) population at 72 h. Moreover, during the course from 48 to 72 h, a decrease of polyploid cells and a reciprocal increase of sub-G_1 population were associated with each other, indicating that the arrested K562 cells entered into apoptosis. An important feature of apoptosis is the fragmentation of genomic DNA into integer multiples of 180-bp units, resulting in a characteristic ladder on agarose gel electrophoresis. Fig. 5A showed the typical DNA fragmentation when K562 cells were treated with methyl protodioscin for 72 h. In addition, the annexin V binding assay was performed to detect the transverse redistribution of plasma membrane phosphatidylserine, which is a hallmark of early apoptotic cells. Fig. 5B shows the FACS histogram with dual parameters including annexin V-FITC and SSC (side scatter), which is a marker of cell granularity. In untreated K562 cells, only 4.82% cells were annexin V-positive. After treated with 3 μM methyl protodioscin for 48 h, the positive cells increased to 52.05%. Significantly, most of these apoptotic cells (34.16%) had more granularity in the nucleus, indicating that they derived from G_2/M

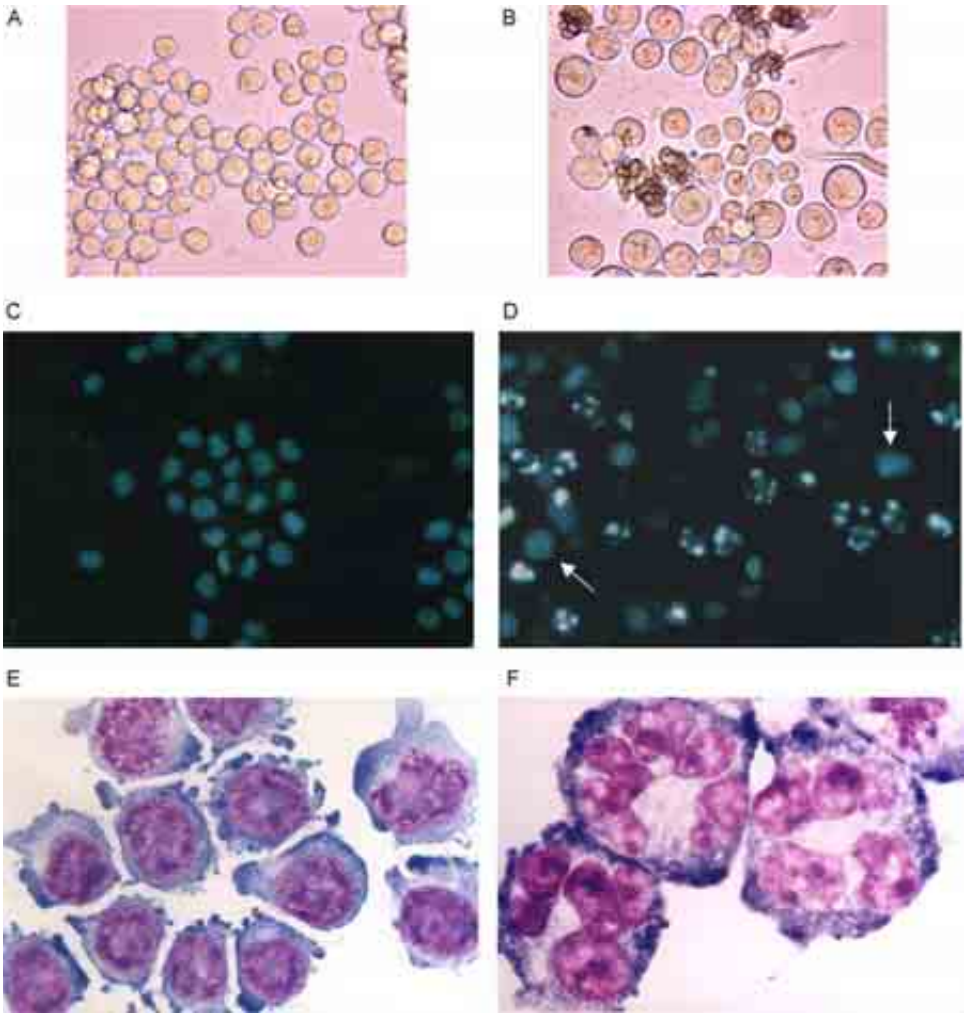

Fig. 3. Morphological changes of K562 cells when treated with 3 μM methyl protodioscin for 48 h. (A) and (B) phase-contrast microscopic view; (C) and (D) fluorescence microscopic view; (a and c, untreated cells; b and d, methyl protodioscin-treated cells). The condensed chromatin is seen as spot in the nucleus by DAPI staining; multinuclear cells are shown with arrowheads, magnification ×400. (E) and (F) Wright-Giemsa staining of untreated and methyl protodioscin-treated cells, magnification ×1000.

arrested cells because cell granularity is proportional to the degree of nuclear complexity.

Since K562 cells lack functional p53 [17], the effects of methyl protodioscin on p53-positive NB_4 cells were investigated. Its treatment caused significant apoptosis in NB_4 cells. Fig. 6A shows the morphological changes including the condensed and fragmented chromatin. Flow cytometric analysis showed the appearance of sub-G_1 cells without obvious cell cycle arrest (Fig. 6B).

Fig. 5 Methyl protodioscin induces apoptosis of K562 cells in a time-dependent manner. (A) K562 cells were treated with 3 μM methyl protodioscin for the indicated times. Apoptosis was evaluated by the induction of DNA fragmentation. (B) Flow cytometric analysis of phosphatidylserine externalization (annexin V binding, FL1-H) and cell granularity (SSC-H). K562 cells were treated with methyl protodioscin (3 μM) for indicated times.

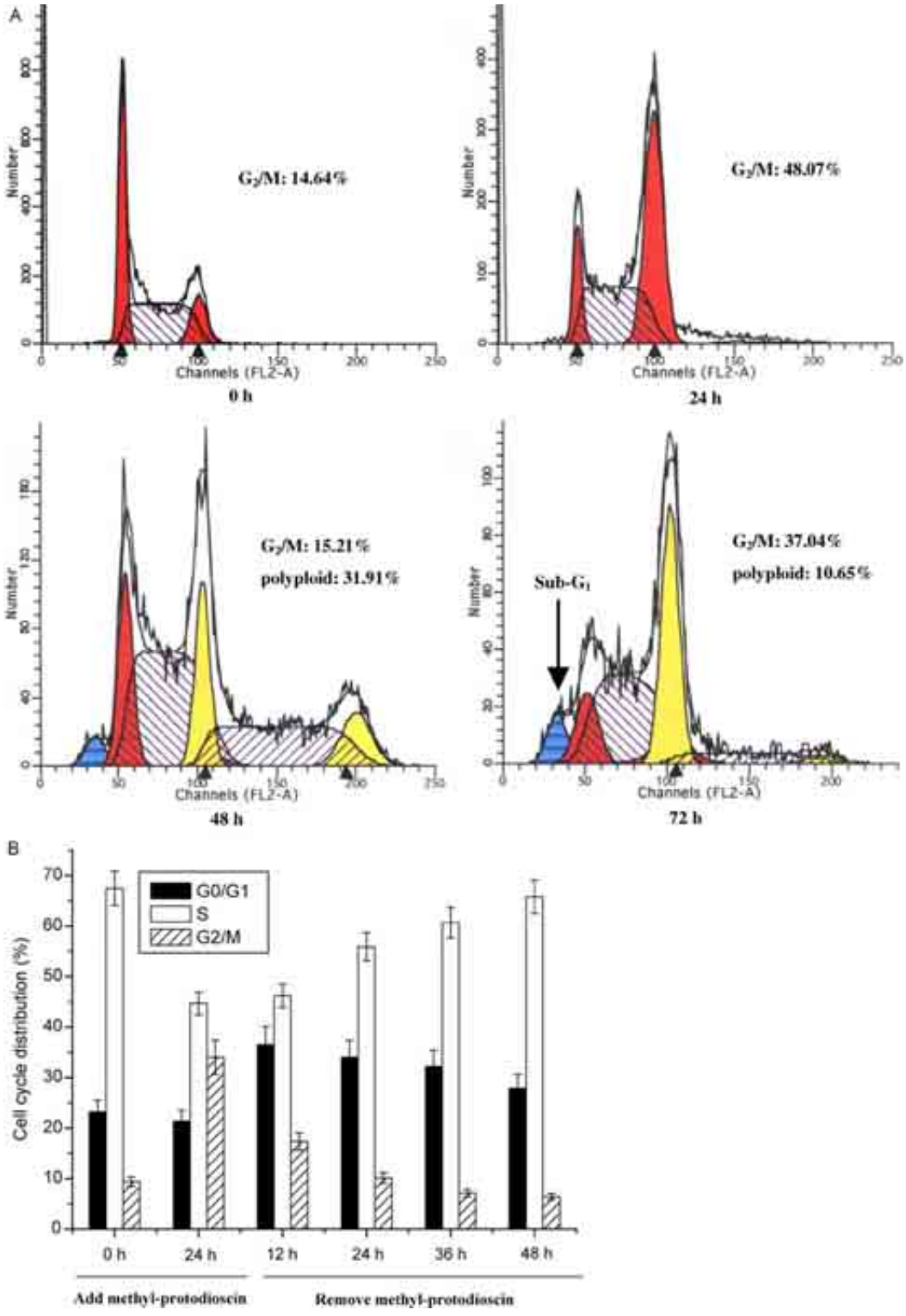
A
Number
Channels (FL2-A)
G2/M: 14.64%
0 h
G2/M: 48.07%
24 h
G2/M: 15.21%
polyploid: 31.91%
48 h
Sub-G1
G2/M: 37.04%
polyploid: 10.65%
72 h
B
G0/G1
S
G2/M
Cell cycle distribution (%)
0 h
24 h
12 h
24 h
36 h
48 h
Add methyl-protodioscin
Remove methyl-protodioscin

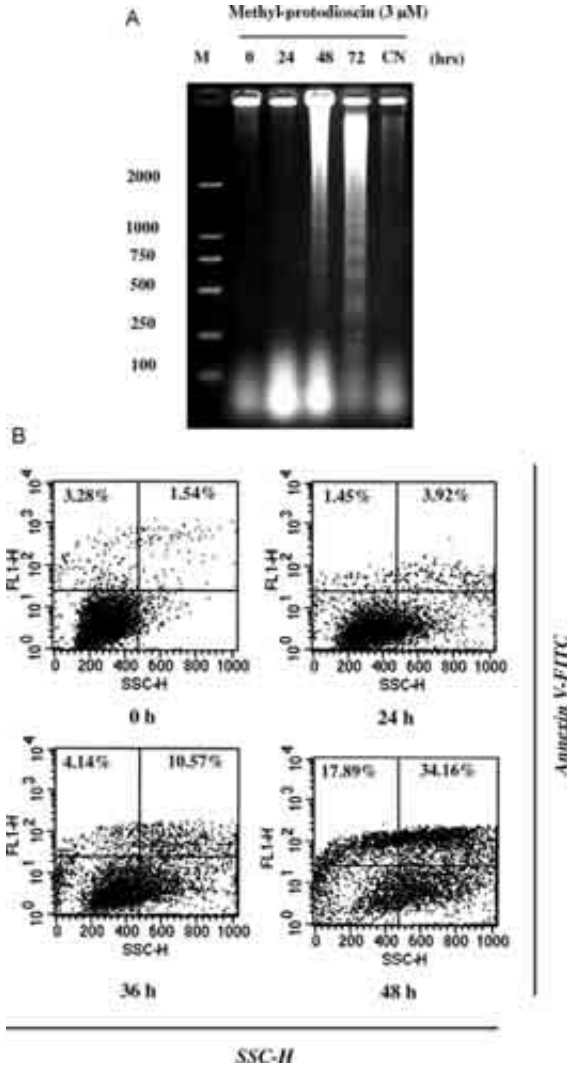

Fig. 5. Methyl protodioscin induces apoptosis of K562 cells in a time-dependent manner. (A) K562 cells were treated with 3 μM methyl protodioscin for the indicated times. Apoptosis was evaluated by the induction of DNA fragmentation. (B) Flow cytometric analysis of phosphatidylserine externalization (annexin V binding, FL1-H) and cell granularity (SSC-H). K562 cells were treated with methyl protodioscin (3 μM) for indicated times.

Cyclin B1-Cdc2 is known to be critical for G_2/M transition and their expression levels were determined by Western blot (Fig. 7). Compared with β-actin control, methyl protodioscin decreased the levels of cyclin B1 in a time-dependent manner, which correlated with cell cycle arresting process. In addition, there is an immunoreactive band above cyclin B1. It is suspected to be a protein complex containing cyclin B1. The expression of Cdc2 kept at a steady level during the whole process.

3.3. Effects of methyl protodioscin on Bcl-2 family members

Western blot was performed to estimate the intracellular levels of Bcl-2 family members when K562 cells were treated with methyl protodioscin. Fig. 7 shows the representative results of Bcl-x_L and Bax. After normalization with reference to β-actin, the levels of Bcl-x_L transiently increased in the period from 24 to 48 h, and then decreased at 72 h. However, the pro-apoptotic Bax levels significantly increased when the cells were treated for 60 or 72 h.

3.4. Methyl protodioscin induces the hyperpolarization of mitochondria, with the loss of MMP as a secondary response

The process of $\Delta\Psi_m$ increase was observed when the cells were treated for 60 h. It was called as mitochondrial hyperpolarization (Fig. 8). At 72 h, the hyperpolarization peak decreased, whereas the peak of depolarization increased. The depolarization corresponds to the lower fluorescence and accounts for the collapse of inner mitochondrial membrane, indicating the dysfunction of mitochondria. It was the point of no return during the commitment stage of apoptosis, suggesting that apoptosis induced by methyl protodioscin was mainly through mitochondrial pathway.

3.5. Methyl protodioscin induces the decline of intracellular Ca^{2+} concentration and the generation of ROS in K562 cells

The treatment of methyl protodioscin reduced the intracellular Ca^{2+} levels as early as 12 h, indicating the decline of intracellular Ca^{2+} concentration was an important initial step for cell cycle arrest and apoptosis (Fig. 9A). The intensity of Fluo-3 fluorescence kept at a low level from 12 to 48 h, and increased after that. It is suspected that the latter reconversion of Ca^{2+} concentration was essential for the progression of apoptosis. The concentration of ROS that was determined by DCFH-DA fluorescence,

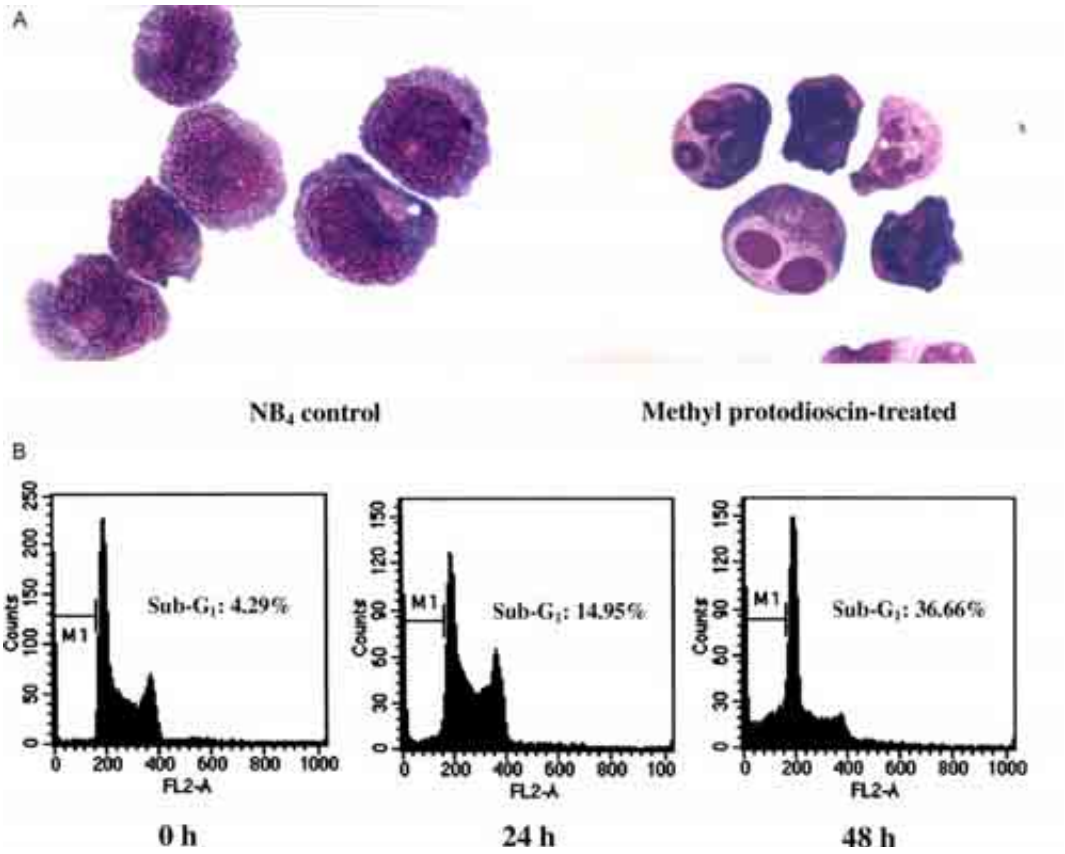

Fig. 6. Effects of methyl protodioscin on human leukemia NB_4 cells. (A) Morphological changes of NB_4 cells when treated with 5 μM methyl protodioscin for 48 h. Microscopic pictures were taken when the cells were dyed with Wright-Giemsa stain, magnification ×1000. (B) Cell cycle profile and the appearance of sub-G_1 cells (M1) when NB_4 cells were treated with 5 μM methyl protodioscin for the indicated times.

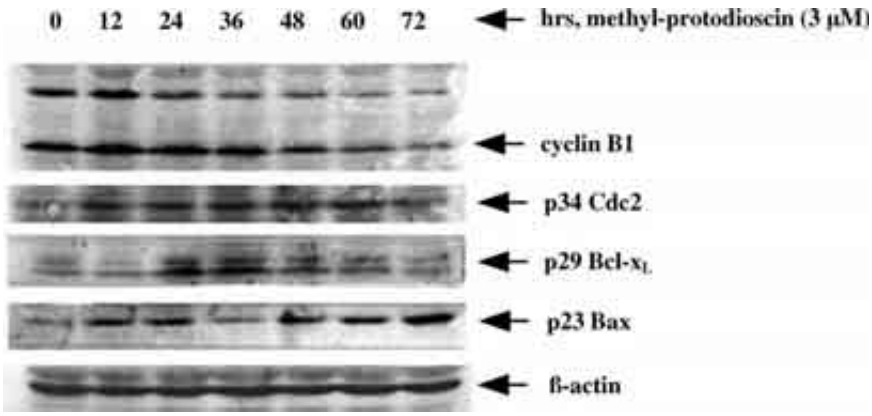

Fig. 7. Effects of methyl protodioscin on mitosis and apoptosis-associated proteins in K562 cells. Western blot analysis of Cdc2, cyclinB1, Bcl-x_L and Bax levels in the lysates from untreated and methyl protodioscin-treated K562 cells. β-actin was used as an internal control to normalize the amounts of proteins loaded in each lane.

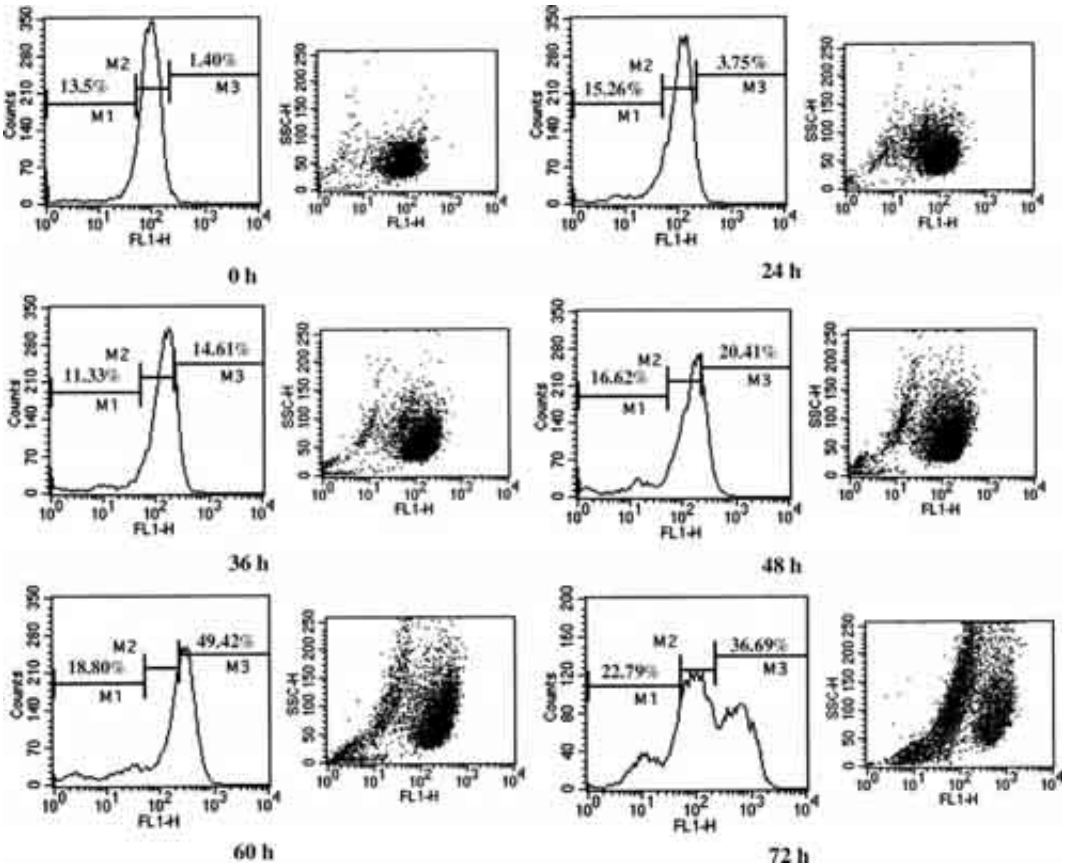

Fig. 8. Time course analysis of MMP in the process of methyl protodioscin-induced G_2/M arrest and apoptosis. K562 cells were treated with 3 μM methyl protodioscin for the indicated times. The MMP changes were determined by $DioC_6(3)$ fluorescence with FACS.

increased in a time-dependent manner, suggesting that the continuous generation of ROS was involved in the whole process (Fig. 9B).

4. Discussion

Saponins are a structurally and biologically diverse class of glycosides of steroids and triterpenes in secondary metabolites, which is one of the most promising sources of leads in drug discovery. The present study clearly demonstrates that methyl protodioscin initiates a series of events leading to G_2/M arrest and apoptosis, such as cyclin B1 down-regulation, Ca^{2+} homeostatic perturbation, mitochondrial dysfunction, and ROS generation.

Cell cycle kinetic studies revealed that the blockade of G_2/M progression is a requisite step for the subsequent apoptosis (Fig. 4). It is not fully understood how methyl protodioscin causes K562 cells to undergo G_2/M arrest and apoptosis. Previous study described this phenomenon as the development of an aberrant mitotic exit into G_1-like 'multinucleate state', which eventually progressed into apoptosis [18]. Our speculation is that methyl protodioscin may either interact with microtubule, resulting in the interruption of its assembly, or induces the inappropriate alteration in the expression and/or activation of CDKs and their regulators. This arresting effect can be reversed with drug removal, which may be due to reversible drug binding or restored cell signaling changes. The suppression of cyclin B1, which is

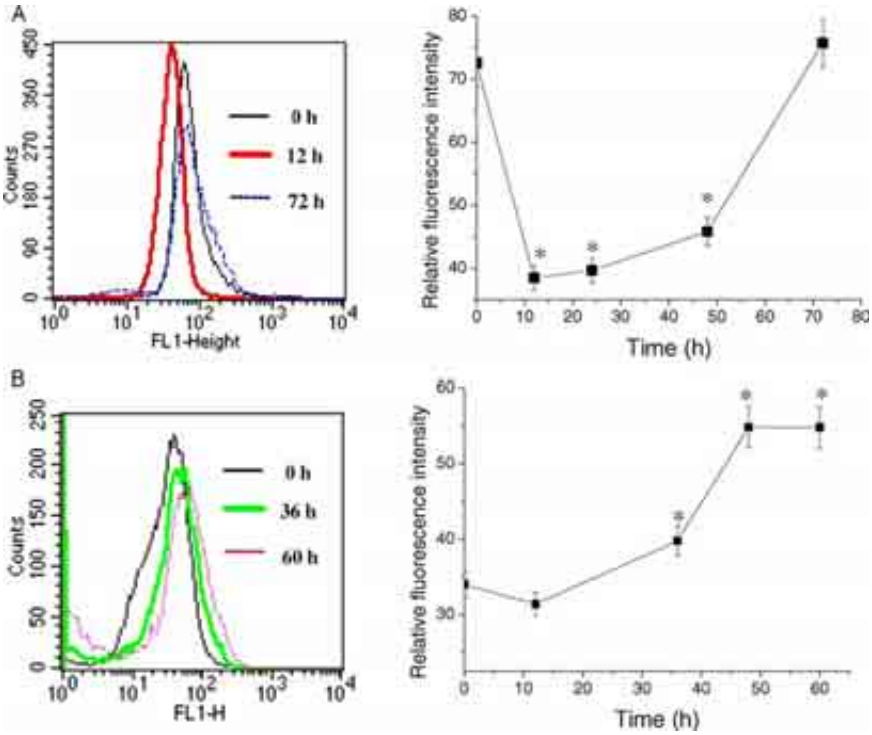

Fig. 9. Effects of methyl protodioscin on cytoplasmic Ca^{2+} concentration and ROS generation in K562 cells. (A) K562 cells were treated with 3 μM methyl protodioscin for the indicated times. The intracellular Ca^{2+} concentration was determined by the fluorescenct activity of Fluo-3 with FACS. (B) K562 cells were treated with 3 μM methyl protodioscin for the indicated times. The ROS generation was determined by the DCFH-DA fluorescence with FACS.

the regulatory subunit of the Cdc2 kinase, should be due to the G_2/M arresting effects (Fig. 7). Since the degradation of cyclin B1 determines the completion of mitosis, K562 cells might be arrested at G_2 rather than M phase. Innocente et al. [19] reported that p53 arrested cell cycle at G_2/M phase by lowering cyclin B1 levels, which challenges our observation because K562 cells are deficient in functional p53 [17]. The observed multinucleation phenotype represents additional rounds of DNA replication, indicating that negative p53 cannot prevent the damaged cells re-into cell cycle. Methyl protodioscin-induced apoptosis without cell cycle arrest in p53-positive NB_4 cells, indicating it has different effects on the two cell lines point to p53-dependent and p53-independent regulation of cell cycle.

Mitochondrial homeostasis plays a pivotal role in regulating apoptosis. Pro-apoptotic signals (i.e. ROS, altered redox status, and increased Ca^{2+} levels) can trigger the mitochondria to release caspase-activating proteins into cytosol, such as cytochrome *c*, AIF and Smac/DIABLO, subsequently committing the cell to die by Apaf-1-mediated activation of the caspase-9 and caspase-3. One of the early events is the alteration of the integrity of mitochondrial membranes consisting of inner and outer membrane. MMP ($\Delta\Psi_m$) is generated by the respiratory chain or through ATP-dependent reversal of mitochondrial ATP synthase. Its maintenance is crucial to a number of mitochondrial functions, such as ATP production, and homeostasis of intramitochondrial Ca^{2+} levels. In this study, we observed the increase of MMP during the stage of cell cycle arrest. Mitochondrial hyperpolarization, as described by other authors for other cell types [20,21] seem to represent a prerequisite for rapid mitochondria-mediated

apoptosis that eventually leads to the loss of MMP. These hyperpolarization effects can result from different actions, such as an increased mitochondrial mass and number per cell or an increase in matrix volume [22], the latter leading to swelling and rupture of the outer membrane, followed by a decrease of $\Delta\Psi_m$. As shown in Fig. 8, the initial increase of $\Delta\Psi_m$ in K562 cells is consistent with the arrest of the cells in G_2/M phase and the subsequent disruption of $\Delta\Psi_m$ is associated with the appearance of hypo-diploid DNA content peak. Maybe the mitochondrial hyperpolarization is attributable to the G_2/M-phase cells and the depolarization to the apoptotic cells, as indicated in the dual parametric dot plots combining cell granularity (SSC-H) and $DiOC_6(3)$ fluorescence (FL-1). Methyl protodioscin may have a deleterious effect on the electron transport chain because the hyperpolarization can also be driven by respiration increase, as a result of enhanced oxidative phosphorylation and ATP production [23]. The increase of MMP can hold the electron carriers of the respiratory chain in a much reductive state, which makes ROS more easily released [24]. The burst of ROS in cytosol might act as a mediator in apoptotic pathways and in turn act on MMP. Mitochondrial Ca^{2+} accumulation and increased ROS production finally lead to irreversible damage to mitochondria and the triggering of the cell death.

The anti-apoptotic Bcl-x_L has been shown to exert its inhibitory effects on apoptosis by blocking the release of cytochrome *c* and the decline of MMP [25]. The present results showed that its up-regulation is consistent with G_2/M arrest while its down-regulation in line with the subsequent apoptosis (Fig. 7). Over-expression of Bcl-x_L and abrogation of p53 cooperate to allow rapid and progressive polyploidization following mitotic spindle damage [26], which is associated with the multinucleated phenotype observed in the cells treated with methyl protodioscin. Bax, a multidomain pro-apoptotic cytosolic protein, integrates to the outer mitochondrial membrane and causes cytochrome *c* release [25]. Its increased level at 72 h contributes to the additional observation that Bax membrane insertion is a late event in the process. Furthermore, Bax involves direct effect on sensitization of mitochondria to Ca^{2+}-mediated fluxes and cytochrome *c* release [27]. The changes of Bcl-x_L and Bax coincide with the restoration of intracellular Ca^{2+}, indicating their roles in regulating Ca^{2+} flow.

Methyl protodioscin induced a dramatic decline of cytoplasmic Ca^{2+} concentration (Fig. 9A). Two hypotheses are proposed to explain the involvement of Ca^{2+} in the process of G_2/M arrest and apoptosis. The first one is that methyl protodioscin, as a detergent, might have an ill effect on membrane lipid composition, resulting in the efflux of Ca^{2+}. The second hypothesis is that the rapid decrease of intracellular Ca^{2+} is predominantly the result of stimulation on Ca^{2+} uptake of mitochondria, which is a major feature of cell injury. This process requires oxidative phosphorylation and is energy-dependent, which may have benefited from the increased $\Delta\Psi_m$, because the uptaking process by the uniporter is driven by negative MMP [28]. The maintenance of a normal $\Delta\Psi_m$ is crucial to the homeostasis of intramitochondrial Ca^{2+} level. And changes in $\Delta\Psi_m$ were correlated to fluctuations in cytosolic Ca^{2+}. Our results establish a close relationship between the alterations of Ca^{2+} concentration and MMP in affected cells. The Fluo-3 fluorescence had dropped below control from 12 to 48 h, while there was an elevation in $DioC_6(3)$ fluorescence. When K562 cells showed clear morphology of apoptosis at 72 h, $\Delta\Psi_m$ decreased while cytosolic Ca^{2+} concentration was restored. It is speculated that the initial mitochondrial hyperpolarization was an immediate reaction to Ca^{2+} down-regulation; the latter intracellular increase of Ca^{2+} concentration was directly related to the loss of MMP. The restored cytosolic Ca^{2+} may serve to release apoptogenic proteins from mitochondria, trigger the production of ROS, and activate apoptosis-related proteases. Recent findings have provided ample evidence for crosstalk between Ca^{2+} signaling, calpains, caspases and other protease families [11].

In conclusion, methyl protodioscin causes G_2/M arrest and apoptosis in human leukemia K562 cells. Intracellular Ca^{2+} fluctuation is a pivotal event that leads to mitochondrial dysfunction, with the hyperpolarization as a remarkable characteristic in the whole process. Additionally, the treated cells arrest at a specific point (G_2 point) in the cell cycle, indicating the formulation of a specific, programmed signaling response. This study provides a mechanistic

background for the introduction of this potent leading compound in cancer chemotherapy.

Acknowledgements

This work was supported in part by grants from the exchange research program of Hong Kong Baptist University. We also thank Professor Yong Ju, Department of Chemistry, Tsinghua University, for kindly providing methyl protodioscin.

References

[1] R.W. Johnstone, A.A. Ruefli, S.W. Lowe, Apoptosis: a link between cancer genetics and chemotherapy, Cell 108 (2002) 153–164.
[2] E.A. Sausville, Y. Elsayed, M. Monga, G. Kim, Signal transduction-directed cancer treatments, Annu. Rev. Pharmacol. Toxicol. 43 (2003) 199–231.
[3] S.J. Elledge, Cell cycle checkpoints: preventing an identity crisis, Science 274 (1996) 1664–1672.
[4] D. Arion, L. Meijer, L. Brizuela, D. Beach, Cdc2 is a component of the M phase-specific histone H1 kinase: evidence for identity with MPF, Cell 55 (1988) 371–378.
[5] D.R. Green, J.C. Reed, Mitochondria and apoptosis, Science 281 (1998) 1309–1312.
[6] S. Desagher, J.C. Martinou, Mitochondria as the central control point of apoptosis, Trends Cell. Biol. 10 (2000) 369–377.
[7] X. Jiang, X. Wang, Cytochrome *c* promotes caspase-9 activation by inducing nucleotide binding to Apaf-1, J. Biol. Chem. 275 (2000) 31199–31203.
[8] S. Cory, J.M. Adams, The Bcl-2 family: regulators of the cellular life-or-death switch, Nat. Rev. Cancer 2 (2002) 647–656.
[9] M. Crompton, The mitochondrial permeability transition pore and its role in cell death, Biochem. J. 341 (1999) 233–249.
[10] M.R. Duchen, Contributions of mitochondria to animal physiology: from homeostatic sensor to calcium signaling and cell death, J. Physiol. 516 (1999) 1–17.
[11] S. Orrenius, B. Zhivotovsky, P. Nicotera, Regulation of cell death: the calcium-apoptosis link, Nat. Rev. Mol. Cell Biol. 4 (2003) 552–565.
[12] K. Hu, A. Dong, X. Yao, H. Kobayashi, S. Iwasaki, Antineoplastic agents; I. Three spirostanol glycosides from rhizomes of *Dioscorea collettii* var. *hypoglauca*, Planta Med. 62 (1996) 573–575.
[13] K. Hu, X.S. Yao, Protodioscin (NSC-698 796): its spectrum of cytotoxicity against sixty human cancer cell lines in an anticancer drug screen panel, Planta Med. 68 (2002) 297–301.
[14] J. Yin, Y. Tezuka, K. Kouda, Q.L. Tran, T. Miyahara, Y.J. Chen, S. Kadota, In vivo antiosteoporotic activity of a fraction of *Dioscorea spongiosa* and its constituent, 22-*O*-methylprotodioscin, Planta Med. 70 (2004) 220–226.
[15] M.S. Cheng, Q.L. Wang, Q. Tian, H.Y. Song, Y.X. Liu, Q. Li, et al., Total synthesis of methyl protodioscin: a potent agent with antitumor activity, J. Org. Chem. 68 (2003) 3658–3662.
[16] Z. Wang, J. Zhou, Y. Ju, H. Zhang, M. Liu, X. Li, Effects of two saponins extracted from the *Polygonatum zanlanscianse* on the human leukemia (HL-60) cells, Biol. Pharm. Bull. 24 (2001) 159–162.
[17] M. Lubbert, C.W. Miller, L. Crawford, H.P. Koeffler, p53 in chronic myelogenous leukemia. Study of mechanisms of differential expression, J. Exp. Med. 167 (1988) 873–886.
[18] M.A. Jordan, K. Wendell, S. Gardiner, W.B. Derry, H. Copp, L. Wilson, Mitotic block induced in HeLa cells by low concentrations of paclitaxel (Taxol) results in abnormal mitotic exit and apoptotic cell death, Cancer Res. 56 (1996) 816–825.
[19] S.A. Innocente, J.L. Abrahamson, J.P. Cogswell, J.M. Lee, p53 regulates a G_2 checkpoint through cyclin B1, Proc. Natl Acad. Sci. USA 96 (1999) 2147–2152.
[20] P.F. Li, R. Dietz, R. von Harsdorf, p53 regulates mitochondrial membrane potential through reactive oxygen species and induces cytochrome *c* independent apoptosis blocked by bcl-2, Eur. Mol. Biol. Organ. J. 18 (1999) 6027–6036.
[21] M.G. Vander Heiden, N.S. Chandel, P.T. Schumacker, C.B. Thompson, Bcl-x_L prevents cell death following growth factor withdrawal by facilitating mitochondrial ATP/ADP exchange, Mol. Cell 3 (1999) 159–167.
[22] J.C. Reed, J.M. Jurgensmeier, S. Matsuyama, Bcl-2 family proteins and mitochondria, Biochim. Biophys. Acta—Bioenergetics 1366 (1998) 127–137.
[23] S. Matsuyama, J. Lopis, Q.L. Deveraux, R.Y. Tsien, J.C. Reed, Changes in intramitochondrial and cytosolic pH: early events that modulate caspase activation during apoptosis, Nat. Cell Biol. 2 (2000) 318–325.
[24] K.B. Wallace, J.T. Eells, V.M.C. Madeira, G. Cortopassi, D.P. Jones, Mitochondria-mediated cell injury, Fundam. Appl. Toxicol. 38 (1997) 23–37.
[25] A. Gross, J.M. McDonnell, S.J. Korsmeyer, BCL-2 family members and the mitochondria in apoptosis, Genes Dev. 13 (1999) 1899–1911.
[26] A.J. Minn, L.H. Boise, C.B. Thompson, Expression of bcl-x(L) and loss of p53 can cooperate to overcome a cell cycle checkpoint induced by mitotic spindle damage, Genes Dev. 10 (1996) 2621–2631.
[27] L. Zhu, S. Ling, X.D. Yu, L.K. Venkatesh, T. Subramanian, G. Chinnadurai, T.H. Kuo, Modulation of mitochondrial Ca^{2+} homeostasis by Bcl-2, J. Biol. Chem. 274 (1999) 33267–33273.
[28] G. Kroemer, B. Dallaporta, M. Resche-Rigon, The mitochondrial death/life regulation of apoptosis and necrosis, Annu. Rev. Physiol. 60 (1998) 619–642.